COMPUTER VISION AND IMAGE UNDERSTANDING
Vol. 69, No. 2, February, pp. 156–169, 1998
ARTICLE NO. IV970598

Pruning Medial Axes

Doron Shaked* and Alfred M. Bruckstein†

Center for Intelligent Systems, Technion, Haifa 32000, Israel
E-mail: dorons@hp.technion.ac.il, freddy@cs.technion.ac.il

Received May 16, 1996; accepted December 31, 1996

The medial axis is an attractive shape feature; however, its high sensitivity to boundary noise hinders its use in many applications. In order to overcome the sensitivity problem some regularization has to be performed. Pruning is a family of medial axis regularization processes, incorporated in most skeletonization and thinning algorithms. Pruning algorithms usually appear in a variety of application-dependent formulations. Inconsistent terminology used until now prevented analysis and comparison of the various pruning methods. Indeed many seemingly different algorithms are in fact equivalent. In this paper we suggest the rate pruning paradigm as a standard for pruning methods. The proposed paradigm is a framework in which it is easy to analyze, compare, and tailor new pruning methods. We analyze existing pruning methods, propose two new methods, and compare the methods via a model-based analysis. The theoretical analysis is supported by simulation results of the various pruning methods. © 1998 Academic Press

1. INTRODUCTION

The medial axis (axis curve and associated radius function) is a mathematically well-defined, easily invertible shape representation, which combines, in a unique way, local boundary information with local region information. The axis curve is a graphlike set in the shape composed of, generally smooth, curve segments joined together in junctions. It constitutes an intuitively appealing homotopic and thin version of the shape [20], and, thus if a shape is simply connected, its axis curve has the graph structure of a tree. These facts may explain why, despite frequent shifts in methods and paradigms, the medial axis has constantly maintained a central role in computer vision and shape analysis research [1, 6, 23, 24, 32, 35, 42].

Using the medial axis for shape analysis has some drawbacks. Most notably, viewed as a transform from the space of simple closed curves (boundary curves of simply connected shapes) to the metric space of tree-graph structures of curves (axis curves), the metric in both spaces being the Hausdorff metric, the medial axis transform is not continuous. In simple words, arbitrarily small boundary fluctuations result in significant changes of the medial axis; see, e.g., Fig. 1. This problem is enhanced due to the fact that irrespective of resolution, digital shapes have an intrinsically rough boundary. It has already been speculated [29, 31] that the technical problems arising from the extended sensitivity to boundary noise play an important role in the reason why, despite the many apparent advantages and the considerable research effort invested in this direction, the use of the medial axis in computer vision is still limited to a small number of applications.

Some skeletonization algorithms (e.g., Voronoi skeletons) yield axes that are often excessively *hairy* if no regularization is performed [4, 8, 28, 33, 34]. We use the term "hairy" to describe noise in the axis domain. The reason for that terminology is that what usually happens to the axis of shapes whose boundary has been affected by noise is that "noisy" axis segments protrude from practically everywhere on the true axis curve to practically everywhere on the boundary, which gives the impression of a "hairy" skeleton.

It was indeed recognized, right from the beginning [23] that in order to overcome the skeleton sensitivity problem, some regularization is necessary, either in the form of preprocessing of the boundary, or directly on the resulting "hairy" axis. Until recently [22], shape and boundary smoothing algorithms were afflicted by topological changes; therefore most regularization procedures were performed on the complete axis or during a thinning operation. Regularization of given axes or during thinning is called *pruning*, since pruning of a hairy tree is indeed called upon.

Pruning is thus an essential part of skeletonization and thinning algorithms, and practically all skeletonization algorithms designed for general shapes implement some type of pruning. Nevertheless, most pruning methods rely on ad hoc heuristic rules, which are invented and often reinvented in a variety of equivalent application-driven formulations. There were only a few attempts in the literature to analyze pruning methods and rules [17, 27–29, 31, 34].

The analysis of pruning is difficult, as is the analysis of other shape regularization methods. Indeed the regularization of medial axes induces an implicit regularization or smoothing of the shape and its boundaries. Thus, the choice of an optimal or even a preferred pruning method is intimately related to a good understanding of boundary smoothness. Since the issues of what are

* Work done while in the Department of Electrical Engineering at the Technion. Hewlett Packard Laboratories Israel, Technion City, Haifa 32000, Israel.
† Department of Computer Science, The Technion, Haifa 32000, Israel.

1077-3142/98 $25.00

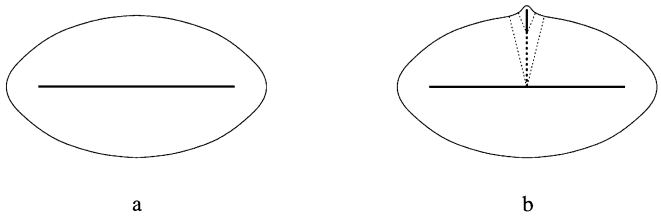

FIG. 1. Small boundary fluctuations result in significant changes of the medial axis.

smooth shapes, and how to perform good shape smoothing are not yet resolved, we are bound to have many pruning methods.

Practically all pruning methods are based on defining an intrinsic significance measure for axis points. Variability in significance measures is the major source for variability in pruning methods. A secondary source of variability follows from different pruning paradigms, i.e. different ways to incorporate the intrinsic significance measures in the pruning process.

The main goal of this paper is to introduce a standard framework for pruning methods, which consists of a specific pruning paradigm and a standard terminology for significance measures. The proposed terminology should be flexible enough to accommodate all reasonable pruning methods, although some of them correspond to irreconcilable interpretations of smoothness. A terminology consistent across all applications will surely enhance the flow of information and enable comparison of different pruning methods.

In this paper we also suggest two new pruning methods the heuristics of which may be regarded, in some contexts, as improvements on existing methods. The suggested methods provide an example of how the proposed paradigm helps in the understanding of pruning methods and in the tailoring of new methods.

Section 2 contains some preliminaries: definitions, terminology issues, and a short discussion of pruning versus shape smoothing. In Section 3 we briefly review pruning methods. In Section 4 we introduce three requirements for acceptable pruning techniques. In Section 5 we suggest a pruning paradigm and a standard terminology for significance measures that can accommodate all previously suggested acceptable pruning methods as well as several others. Then using the proposed paradigm and terminology, we introduce two new pruning methods in Section 6, and analyze them both theoretically and through simulations in Section 7. We conclude with a summary in Section 8.

2. PRELIMINARIES

2.1. Definitions and Terminology

The medial axis Maximal disks in a planar shape are disks in the shape not contained in any other disk in that shape. The medial axis curve of a planar shape is the locus of centers of maximal disks in that shape. The medial axis is composed of the axis curve and an associated radius function, defined on the axis curve, whose value is the radius of the corresponding maximal disk [6]. In an equivalent definition of the medial axis, known as the Prairie Fire model, one considers a fire front initiated simultaneously on all the boundaries and propagating with constant speed inside the shape. In this context, the medial axis curve is the locus of points where fire fronts originating from different boundary points meet. The radius function, called the quenching function in this model, is the time at which the fire front reaches the quenching point [6]. Other equivalent definitions of the medial axis may be found, e.g., in [23].

Pruning It can be shown [40] that it is difficult to determine medial axis modification rules, in the sense that practically any perturbation in the location of the axis curve or the value of the radius function may result in an illegal axis function, i.e., an axis-like description which does not correspond to any planar shape. The only simple modification rules of legal axes for which axis representations remain legal are: a uniform reduction of the values of the radius function (an operation known as morphological erosion [41]) and arbitrary deletions of axis segments that maintain axis connectivity. All pruning methods amount to various strategies for deletion of "superfluous axis branches."

Skeletonization and thinning In this work we refer to both skeletonization and thinning algorithms. In the literature the terminology is sometimes ambiguous. The usual distinction between skeletonization and thinning is the following: The purpose of skeletonization algorithms is to produce the exact medial axis, whereas thinning algorithms aim at producing "thin versions" of the shape and take the definition and properties of the medial axis only as directional pointers as to how this goal should be achieved. As a result in most thinning algorithms the width information is not retained.

2.2. Pruning versus Shape Smoothing

Curvature flow smoothing [22] appears to gain wide acceptance in the computer vision community as a standard method for smoothing planar shapes. In the Curvature Flow model [13, 16, 22, 30, 38] each boundary point moves in the direction of the normal to the curve, with a velocity proportional to the curvature. It has been shown that in this flow boundaries do not intersect (i.e., shapes maintains their topology), star-shaped shapes remain star-shaped, all nonconvex shapes become convex, and finally evolve into circles [13, 15, 16]. Furthermore, connections have been made between it and some smoothing techniques which were previously introduced in computer vision [25].

Most problems which seemed to prevent axis regularization by shape smoothing were indeed alleviated by curvature flow smoothing. We maintain, however, that there are still some significant problems which inhibit the universal acceptance of curvature flow for axis regularization.

1. Even after smoothing, thinning will be performed from digitized data (either pixel samples or polygonal approximations of the boundary), so that, unless one resorts to skeletonization

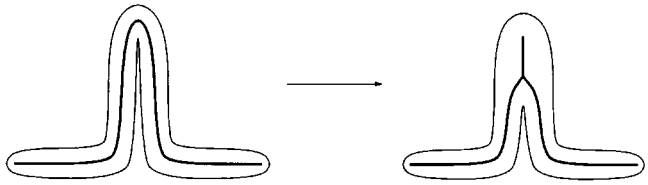

FIG. 2. A new axis segment emerges as a consequence of boundary smoothing.

algorithms from smoothly described boundaries [18, 40], pruning methods will still be necessary.

2. Smoothing of boundaries may result in some undesirable effects on the axis. As in Fig. 2, boundary smoothing may produce new axis segments which may be highly undesired if, for example, the axis is used for length estimation.

3. In all smoothing problems there is an assumption that there exists some scale measure which makes it possible to discern between data and noise; e.g., data has low frequency and noise is high frequency, or data has large shape characteristics, whereas noise is responsible for small details. The problem is that in every scale measure there is usually a significant overlap between data and noise contents. The skeleton pyramid of Ogniewicz [28, 29] specifies two filtering degrees. The axis is pruned strongly and the remaining axis segments are "unpruned" to regain their full original details. This elegant solution of the data/noise detail problem exists only in the axis pruning context.

3. EXISTING PRUNING METHODS

The significance measure used by the earliest pruning methods [6, 12, 23, 36] is the propagation velocity of the symmetry axis in the Prairie Fire model. During the advance of the fire front in the shape, axis points emerge continuously as fire fronts meet. The velocity V_p by which the axis unfolds is easily shown to depend on the angle ϕ between the tangents at the corresponding boundary points. The propagation velocity is

$$V_p = \frac{V_f}{\cos(\phi/2)}, \tag{1}$$

where V_f is the velocity of the fire fronts. The axis propagation velocity varies between the fire propagation velocity when $\phi = 0$ and infinity when $\phi = \pi$; see Fig. 3. Indeed, the angle between generating boundaries of many hairy axis branches is low (see, e.g., the dotted part in Fig. 1b).

The classic pruning paradigm, applied also in most papers using propagation velocity as the significance measure [6, 12, 19, 23, 36] is the threshold paradigm: all axis points whose significance measure is low are deleted. Such pruning may, however, result in disconnected axes, as can be seen in Fig. 1b, where the dotted axis denotes low propagation velocity.

Various improved paradigms were suggested in order to overcome the potential disconnections in the axis. In those paradigms pruning is activated from the end points of the axis branches as long as a certain condition is satisfied. Pruning is performed either while the significance measure is decreasing or while it is below a threshold [2, 4]. However, by making the resulting axis connected, pruning ceases to be continuous; i.e., arbitrarily small changes in the threshold of the significance measure may result in significant changes of the pruned axis. An example of this phenomenon is described in Fig. 4, where the effect of two close threshold levels is depicted on a graph of the significance measure versus axis arc length.

In many thinning algorithms pruning is performed during thinning, by a relaxation of the condition for initializing new axis segments. An axis segment is initialized when during erosion, the curvature at some boundary point becomes significantly large, and thus, if only larger curvatures are considered significant, the initialization condition is relaxed. It is quite clear that in boundary configurations as, for example, in Fig. 3, the local curvature will stay constant during the erosion, its value depending only on the relative angle of the generating boundaries: low curvature in Fig. 3a, and larger in Fig. 3c. We may therefore conclude that in some sense, relaxation of axis initialization conditions through manipulation of curvature significance is similar to pruning according to propagation velocity. In fact, the paradigm of pruning during thinning is similar to pruning paradigms deleting outer axis elements below a certain threshold (see, e.g., [4]).

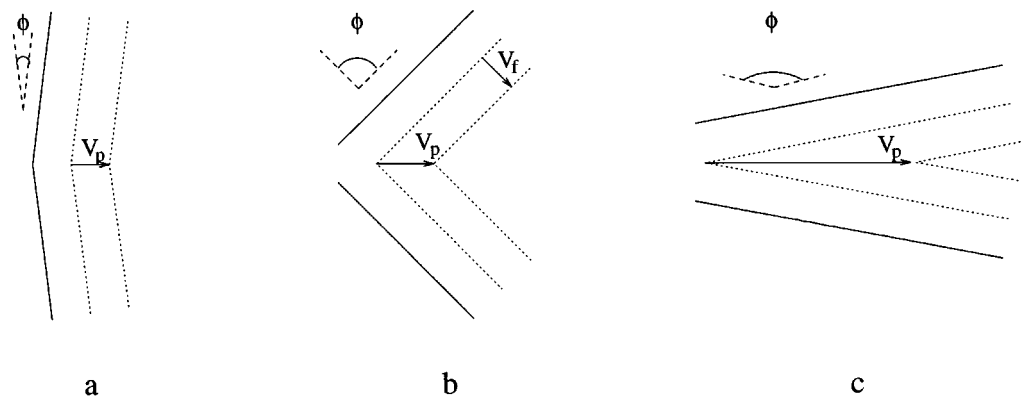

FIG. 3. Propagation velocity depends on the angle between the generating boundaries.

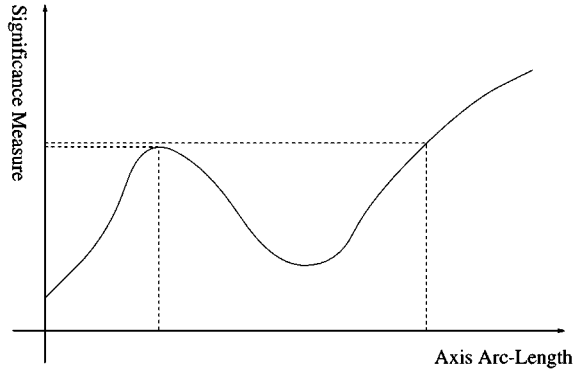

FIG. 4. Two close threshold levels result in significantly different pruning locations.

It has to be noted that, despite the above-mentioned similarity, there is a fundamental difference between pruning of existing axes and pruning during thinning. The decision to assign a pixel to the axis or, alternatively, to erode it has a small local influence on the boundary. Hence, axes resulting from increased pruning levels during pruning are not always exactly included in less pruned axes of the same shape. Still, we argue that it is generally possible and beneficial to unify terminology across this dichotomy of pruning.

A different significance measure is the maximal thickness of the implied erosion [3, 8, 17, 26, 37]. The effect of pruning on the shape is a loss of a localized layer of shape near the boundary, as if the shape has been locally eroded; see Fig. 5. Naturally, one would not want to lose too much shape information in pruning. A possible measure of the amount of shape information lost is the maximal thickness of the eroded layer induced by pruning. Note that for axis segments resulting from boundary perturbations, extensive pruning results in only a limited loss of shape contents.

The thickness of the implied erosion significance measure was used in several application-dependent formulations: The significance measure of a point q on an axis whose endpoint is p is

$$R(p) + d(p, q) - R(q), \tag{2}$$

where $R(\cdot)$ is the radius function on the axis and $d(p, q)$ the

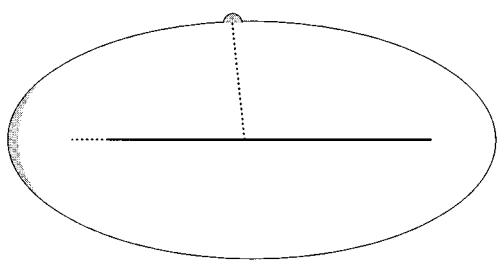

FIG. 5. The effect of pruning on the shape.

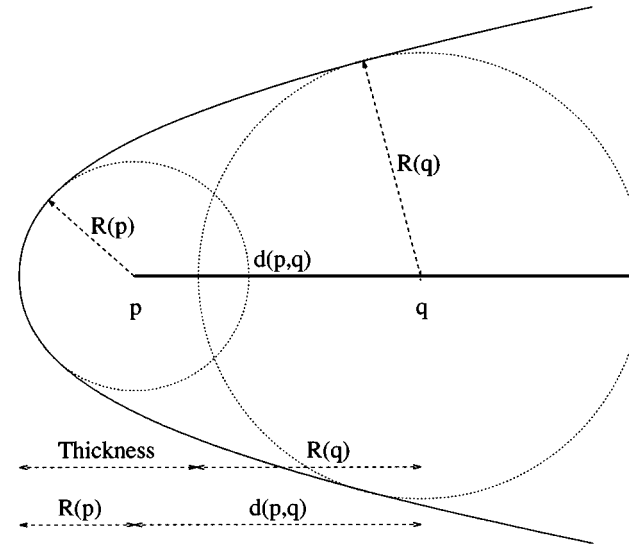

FIG. 6. The erosion thickness significance measure.

distance between points p and q (see Fig. 6). Note that this significance measure is monotone (the radius function $R(q)$ can never increase as much as the distance function d; see, e.g, [6, 35, 40]). Hence, the threshold paradigm can be applied without danger of disconnection.

A different significance measure is related to the length ratio of the axis and the boundary it unfolds: Hairy axis branches may be characterized by the small amount of boundary they unfold (see, e.g., Fig. 1b). In [27–29], Ogniewicz surveys pruning methods and concludes that there are only a few significance measures which can be used in conjunction with a simple thresholding algorithm with no danger of disconnection. Such significance measures viewed as a function over the axis curve have a single local maximum on the axis. Ogniewicz suggests a set of significance measures for which the thresholding approach does not disconnect the axis. All the suggested measures are variations of the boundary/axis length ratio measure, i.e. the amount of boundary unfolded by an axis segment.

Blum and Nagel [7] used a conceptually similar significance measure. They suggested a differential measure $\partial B(a)/\partial a$, where a is the axis arc length parameter and $B(a)$ the length of the boundary unfolded by the axis segment reaching axis point a. Axis significance is determined by integration of the differential significance measure. Note that after integration Blum and Nagel actually prune according to the boundary/axis length ratio measure.

Other significance measures include the radius function and the axis arc length function. In [10] smaller radii are deleted, and in [33] all axis segments are uniformly shortened by a given length (the maximal value of the radius function).

Several pruning methods incorporate boundary smoothing elements into pruning: Arcelli [1] filtered chain codes with triangular weights to induce a scale space over his thinning algorithm. Dill *et al.* [11] used Gaussian weights. Pizer *et al.* [14, 31] used

shape smoothing; consequently they had to deal with changes in shape topology and with axis segments correspondence problems across scales. In [31] they, inevitably, resorted to manual matching of axis segments across scales. (A conceptually similar problem of axis segments correspondence across gray level sets was solved in [14] using active surface models.) Ogniewicz [27] used Gaussian smoothing of axis coordinates [21] and solved the across-scales correspondence problems. In addition to presenting the first truly continuous, fully automatic axis scale space, he also presented a method which indicates the natural scale of the object.

4. ACCEPTABLE PRUNING METHODS

In this section we suggest three rules for acceptable pruning methods, thereby setting the scene for the next section where a pruning paradigm for acceptable pruning methods is presented. We argue that pruning methods that do not comply with the suggested rules are truly unacceptable and, therefore, it is not important whether they may or may not be accommodated in the suggested pruning paradigm.

The rules for acceptable pruning methods are:

1. An acceptable pruning method preserves topology; e.g., it does not disconnect axes.
2. An acceptable pruning method is continuous; i.e., arbitrarily small differences in pruning degree results in arbitrarily small differences in the axes.
3. Significance measures are local on the axis; i.e., it is possible to evaluate the significance from local axis information.

From the short review of the last section it is clear that pruning methods which use fire front propagation velocity as the significance measure are not acceptable, since the corresponding pruning methods are not continuous, or disconnect the axes.

As for the third rule, we chose to include it only because it conceptually limits possible formulations of significance measures to functions of the local axis description (primarily the radius function and its derivatives), the standard terminology we wish to advocate. In the next section we show that the third rule does not, in itself, exclude any existing otherwise acceptable pruning method.

5. STANDARDIZATION OF ACCEPTABLE PRUNING METHODS

In this section we propose a unified terminology for acceptable pruning methods. In the first subsection we present the *rate pruning paradigm* and advocate a specific terminology for significance measures, and in the second subsection we translate some of the existing pruning methods into the proposed standard framework and terminology.

5.1. Standard Paradigm and Terminology

The rate pruning paradigm is a generalization of the pruning method proposed by Blum and Nagel [7]. Instead, of setting a threshold on axial significance the significance measure is used as a cue for the local pruning rate. A high significance measure indicates that pruning should be slow, whereas a low significance measure indicates fast pruning. Rate pruning may be envisioned as a parallel process "melting" the axis simultaneously from all its end points. Formally:

- Pruning is a continuous process in time.
- Pruning is performed on all axis end points in parallel.
- The pruning velocity, or its rate, is determined locally on each branch.
- The pruning rate is inversely proportional to the local significance measure.
  - — Significance measures have to be nonnegative.
  - — If the significance measure is zero, the pruning rate is considered infinite.
- Pruning of a segment terminates when it reaches and annihilates into a junction.
- An annihilating axis segment, merges the remaining two segments at the junction.
- The pruning duration parameterizes the pruning degree.

The rate pruning paradigm assures connectedness and continuity of the pruning, regardless of the incorporated significance measures. Pruning is performed only on axis end points; hence, connectivity is maintained. Discontinuity may only occur if the significance measure becomes zero on a nontrivial axis interval.

In rate pruning, significance measures set the pruning rate. We distinguish them from significance measures which are intended to be used in threshold-based paradigms, and we refer to them as *differential significance measures.*

5.2. Standard Terminology for Existing Methods

In this subsection we formulate the existing acceptable pruning methods within the proposed standard framework and terminology. We start with a standard formulation of a generic acceptable pruning method: Assume we have some acceptable pruning method and we want to find a differential significance measure whose incorporation in the rate-pruning paradigm results in an identical pruning. It is always possible to formulate the desired pruning as the following threshold pruning method: Define the significance measure S of each axis point to be the pruning degree at which the axis point is deleted. Since the desired pruning method is acceptable, the significance measure function has a single local maximum in the entire axis. We want to find the pruning velocity $V(x)$ for every point x on the axis. Note that by our construction

$$S(x) = t(x), \tag{3}$$

where $t(x)$ is the time in which x is pruned. The pruning process should get to point x in time $t(x)$ so that $x = \int^{t(x)} V(\xi)d\xi$, and from (3), $S(\int^t V(\xi)d\xi) = t$. Since S is monotone, it is invertible, and thus $\int^t V(\xi)d\xi = S^{-1}(t)$. Taking the derivative with respect

to t we get

$$V(x) = \frac{\partial}{\partial t} S^{-1}(t)\Big|_{t(x)} = 1 \Big/ \frac{\partial}{\partial x} S(x). \tag{4}$$

We conclude that the differential significance measure required for an equivalent standard pruning is

$$\frac{\partial}{\partial x} S(x), \tag{5}$$

the derivative of the significance measure for threshold pruning.

Let us now formulate the differential significance measure corresponding to pruning by erosion thickness. Given an axis segment, what would be the maximal thickness of the erosion layer induced by deleting a Δ-long segment off its end? In Fig. 6 assume $q = p + \Delta$. If Δ is small enough, we may approximate $R(p) = R(q - \Delta) = R(q) - \Delta \cdot R_a(q)$, where $R_a = \partial R / \partial a$. Replacing $d(p, q) = \Delta$ in (2) we get that the thickness is $\Delta \cdot (1 - R_a(q))$. Hence the differential significance measure corresponding to erosion thickness pruning has the following local formulation:

$$1 - R_a. \tag{6}$$

Note that since $R_a \leq 1$ (see, e.g., [7, 35, 40]), the differential significance measure is indeed nonnegative.

In the basic boundary/axis length ratio pruning suggested by Ogniewicz *et al.* [28, 29], the significance of an axis point is the length of the shortest boundary segment connecting its two generating points. The differential significance measure corresponding to this method was already proposed by Blum and Nagel [7]. In [7, 40] it was shown that the differential length unfolded by the axis is

$$\begin{aligned} l_a &= \left(\frac{1 - R_a^2 - R R_{aa}}{\sqrt{1 - R_a^2}} + K_A R \right), \\ r_a &= \left(\frac{1 - R_a^2 - R R_{aa}}{\sqrt{1 - R_a^2}} - K_A R \right), \end{aligned} \tag{7}$$

where a, l, and r are the arc length parameters of the axis and the boundary segments to its left and right, respectively, R the axis radius function, and K_A is the local axis curvature. Subscripts denote derivatives; e.g., $l_a = \partial l / \partial a$, $R_a = \partial R / \partial a$, and $R_{aa} = \partial^2 R / \partial a^2$. The differential length is depicted in Fig. 7a. The differential significance corresponding to the total boundary length is, therefore,

$$B_a \triangleq l_a + r_a = 2 \frac{1 - R_a^2 - R R_{aa}}{\sqrt{1 - R_a^2}}. \tag{8}$$

It may be shown [40] that the term $1 - R_a^2 - R R_{aa}$ is never negative; hence, (8) is an acceptable differential significance measure.

In [28, 29] Ogniewicz *et al.* propose several length ratio-based significance measures; for example, the chord residual is the difference of the boundary length, $B(a)$, and the length of the chord connecting the two generating points. The length of the local cord is easily shown to be

$$C(a) = 2R\sqrt{1 - R_a^2}. \tag{9}$$

Note [7] that $R_a = \cos\theta$, where θ is the azimuth of the

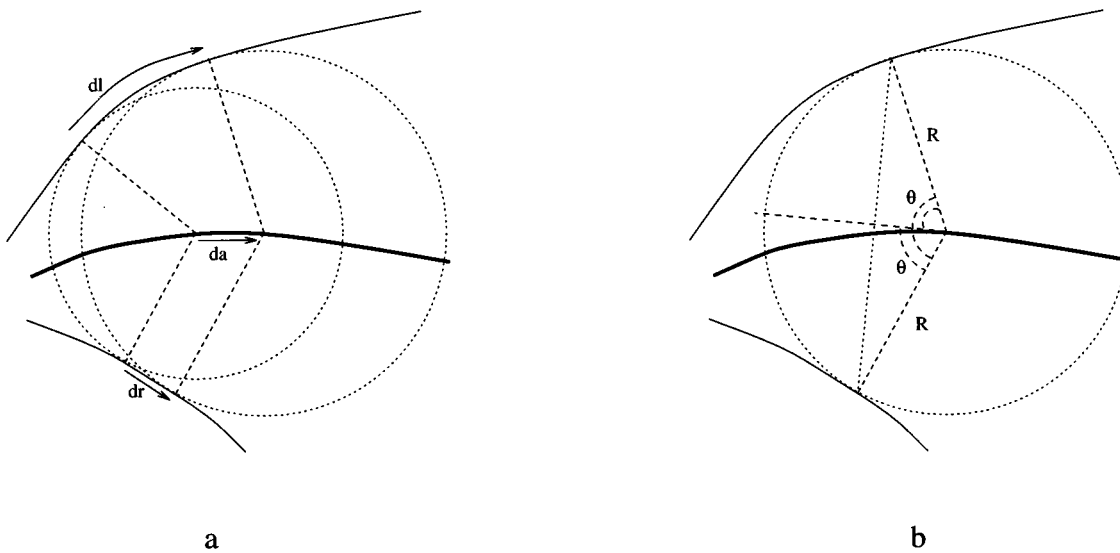

FIG. 7. The differential boundary length (a), and the local chord (b).

generating points measured from the line tangent to the axis (see Fig. 7b).

Differentiating (9), we obtain the differential significance measure corresponding to the chord residual of Ogniewicz *et al.* [28, 29],

$$B_a - C_a = 2(1 - R_a)\frac{1 - R_a^2 - RR_{aa}}{\sqrt{1 - R_a^2}}. \tag{10}$$

Implementing Ogniewicz's residue pruning methods within the rate-pruning paradigm has a small complication of time delays, a phenomenon which has already been observed by Blum and Nagel [7]. Time delays occur when the threshold significance is discontinuous. A step in the threshold significance causes the differential significance to be undefined; however, going back to (4) one can see that the velocity at step discontinuities should be zero for a time period equivalent to the height of the step.

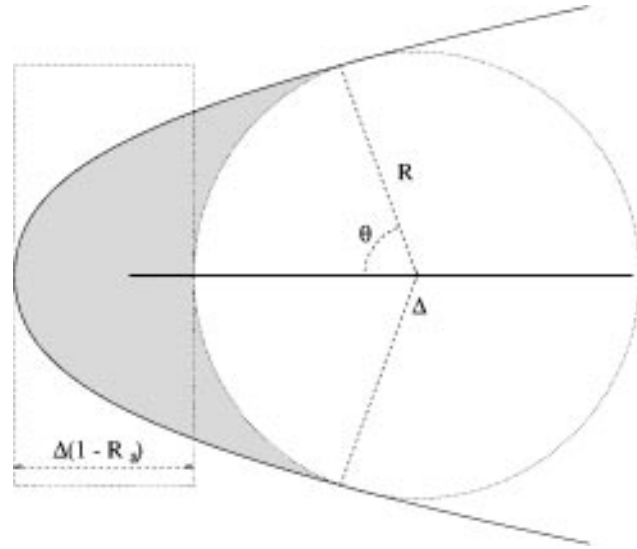

FIG. 8. The differential area and its approximation.

6. NEW PRUNING METHODS

We would have liked to call this section "improved pruning methods" but it would not be correct, since there is no way to determine globally acceptable criteria for pruning quality. We suggest the following pruning methods because they provide an example of how the proposed rate pruning paradigm may help in understanding pruning methods and in tailoring new methods. The proposed methods are, naturally, based on different interpretations of shape smoothness that may, in certain contexts, be regarded as more appropriate than existing methods.

6.1. Erosion Area Pruning

Much the same as in maximal erosion thickness, one can choose the pruned *area* as the significance measure. An area-based significance measure was lately suggested by Attali *et al.* [5], and previously, as context-dependent by Cordella and di Baja [9]. The differential significance measure is the shaded area of the differential crescent in Fig. 8, which as we shall see may be approximated by the area of the rectangle whose height and width are the height $2R\sqrt{1 - R_a^2}$, and maximal thickness $(1 - R_a)$ of the crescent. The proposed erosion area significance measure is, therefore,

$$2R\sqrt{1 - R_a^2} \cdot (1 - R_a). \tag{11}$$

Let us derive the exact formula for the area. Consider the same differential crescent only turned as in Fig. 9. The function describing the top half of a circle is $Z = \sqrt{R^2 - x^2}$. Let the function of the top half of the axis circle Δ close to the axis end point be $Z_1 = \sqrt{R^2 - x^2}$. Approximating the radius at the axis end point by $R - \Delta \cdot R_a$ we get the function of the top half of the axis circle at the axis end point $Z_2 = \Delta + \sqrt{(R - \Delta \cdot R_a)^2 - x^2}$. Note that Z_2 is biased by Δ because the center of the circles are, by our assumptions, Δ apart. A first-order approximation of Z_2 for small Δ gives $Z_2 = \Delta + \sqrt{R^2 - x^2} - R(\Delta \cdot R_a/\sqrt{R^2 - x^2})$ and, hence, $Z_2 - Z_1 = \Delta(1 - RR_a/\sqrt{R^2 - x^2})$. The differential area is $\int (Z_2 - Z_1)_+ \, dx$, where $F(x)_+ = F(x)$, if $F(x) \geq 0$, and 0 otherwise. Since range of $(Z_2 - Z_1)_+$ is $|x| \leq R\sqrt{1 - R_a^2}$, the differential area is

$$\begin{aligned} &2\Delta \int_0^{R\sqrt{1-R_a^2}} \left(1 - \frac{RR_a}{\sqrt{R^2 - x^2}}\right) dx \\ &\quad = 2\Delta R \left(\sqrt{1 - R_a^2} - R_a \sin^{-1}\sqrt{1 - R_a^2}\right). \end{aligned} \tag{12}$$

For small angles (R_a close to 1) we may approximate $\sin^{-1}\sqrt{1 - R_a^2} \cong \sqrt{1 - R_a^2}$, which renders the approximation of (11). For large angles (R_a close to 0) the exact value of $\sin^{-1}$ does not matter, since it is multiplied by R_a. We conclude that the approximation of (11) is reasonable for all R_a.

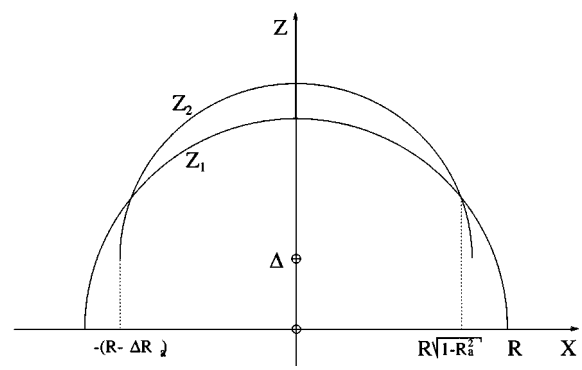

FIG. 9. The functions Z_1 and Z_2.

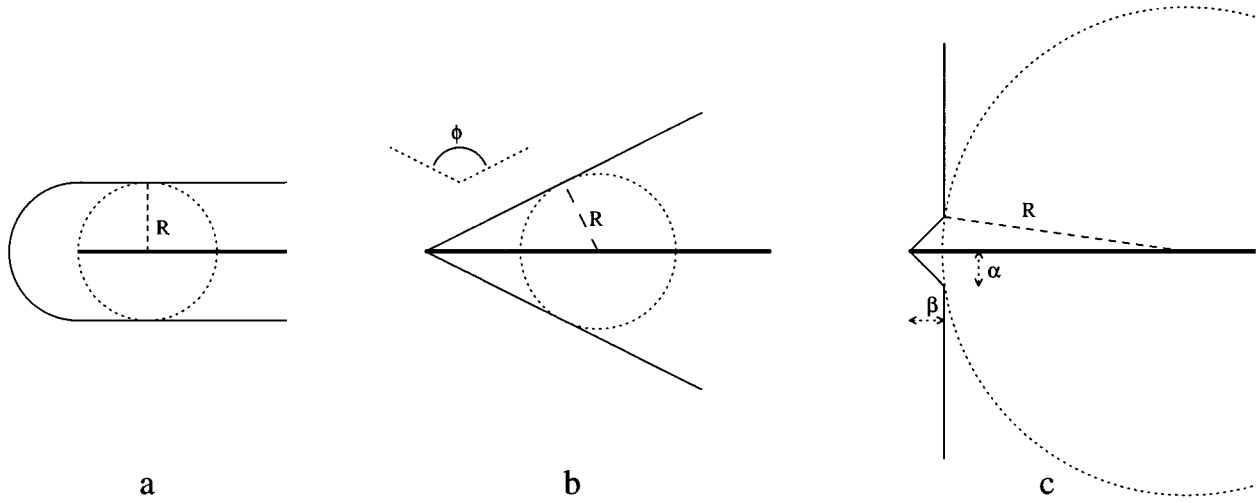

FIG. 10. Axis segment models, (a) constant width, (b) wedge, (c) small perturbation.

6.2. Boundary Smoothing-Based Pruning

In this subsection we propose a new pruning method which is based on boundary smoothing. Previous boundary smoothing-based pruning methods incorporated elements from various shape and boundary smoothing techniques: smoothing of the curvature function [1, 11], shape smoothing [31], and smoothing of the boundary coordinates [27]. We incorporate elements from the curvature flow smoothing [22] which seems recently to gain the position of the preferred shape-smoothing method.

Suppose the boundary of a given shape evolves under a given differential flow. The changing boundary induces a constant change in the shape and its medial axis. Although smooth boundary evolution does not guarantee smooth axis evolution, discontinuities in the axial description are localized both in space and time. In [39] a framework has been suggested to translate differential boundary evolution rules to evolution rules of the axis description. Evolving axes are described by a large set of rules: A curve evolution rule for the axis curve, a rule for the radius function, and boundary rules for both the axis curve and the radius function at free axis end points, as well as at junctions.

It may be shown [39] that when the boundary evolves under curvature flow, axis end points get deleted at a rate proportional to

$$-\frac{1}{R_{aa}R^2}. \tag{13}$$

In addition, the boundary condition for the radius function is

$$R_a = 1. \tag{14}$$

Thus, at the endpoint R_a gets the maximal possible value (it is always true that $|R_a| \leq 1$) and R_{aa} is nonpositive. Hence, the rate (13) is, as required, nonnegative.

A straightforward interpretation of (13) as if the differential significance measure should be $-1/R_{aa}R^2$ is wrong since we ignore (14), and thus we can get, for example, negative significance measures, where the local R_{aa} is positive. We, therefore, approximate R_{aa} to be proportional to the difference between the value of the local R_a and its value at the endpoint where $R_a = 1$, $R_{aa} \cong (R_a - 1)/\Delta a$. Since we want the approximation to be scale invariant, we have to make Δa proportional to the scale. The local scale is determined by the radius function (see also [17]); therefore, we approximate $R_{aa} \sim (R_a - 1)/R$. The resulting pruning rate is $1/(1 - R_a)R$, and the corresponding differential significance measure is

$$R(1 - R_a). \tag{15}$$

It is interesting to note that this significance measure is in some sense halfway between the erosion thickness and the erosion area significance measures (6), (11).

7. ANALYSIS AND RESULTS

In this section we analyze and compare simulation results from different pruning methods: erosion thickness, boundary/axis length ratio, erosion area, and boundary smoothing-based pruning. In Subsection 7.1 we analyze results on a model shape, and in Subsection 7.2 we compare simulation results of general shapes.

7.1. Model-Based Analysis

The significance measures of all the above-mentioned pruning methods depend only on the radius function.[1] Hence it is sufficient to compare their behavior on straight axes. We analyze and compare the pruning methods using the constant width, wedge, and small perturbation axis models (see Fig. 10). In

[1] There is no theoretical restriction prohibiting the use of local axis curve features in significance measures.

the small perturbation model we analyze only the asymptotic behavior.

The wedge and the small perturbation models are two common models for boundary noise, and the constant width model is a good model to study the scale dependence of the pruning methods. The analysis of the models is based on the significance measures derived from the radius functions of the modeled axes.

In the constant width model,

$$R(a) = R \quad \Rightarrow \quad R_a = R_{aa} = 0. \tag{16}$$

In the wedge model,

$$R(a) = a\cos\frac{\phi}{2} \quad \Rightarrow \quad \begin{cases} R_a = \cos(\phi/2) \\ R_{aa} = 0. \end{cases} \tag{17}$$

In the small perturbation model,

$$\begin{aligned} R(a) &= \sqrt{(a-\beta)^2+\alpha^2} \cong a-\beta \\ &\Rightarrow \begin{cases} R_a = \dfrac{1}{\sqrt{1+(\alpha/(a-\beta))}} \cong 1 - \dfrac{\alpha^2}{2(a-\beta)^2} \\ \sqrt{1-R_a^2} \cong \dfrac{\alpha}{a-\beta} \\ R_{aa} = \dfrac{a^2}{\sqrt{(a-\beta)^2+\alpha^2}^3} \cong \dfrac{\alpha^2}{(a-\beta)^3}, \end{cases} \end{aligned} \tag{18}$$

where the approximations are for large a values ($a \gg \alpha$).

We arrive at a description of the differential significance measures of the axes as a function of the model parameters and possibly the axis arc length. The different significance measures are summarized in Table 1.

To support the analysis we present some simulation results. The input shape contains all the above-mentioned axis models. It has two constant-width axis segments having different width scales, two wedge segments with different opening angles ϕ, a small perturbation segment, and an inward depression feature. The inward depression feature is the shapebackground dual of the small perturbation feature.

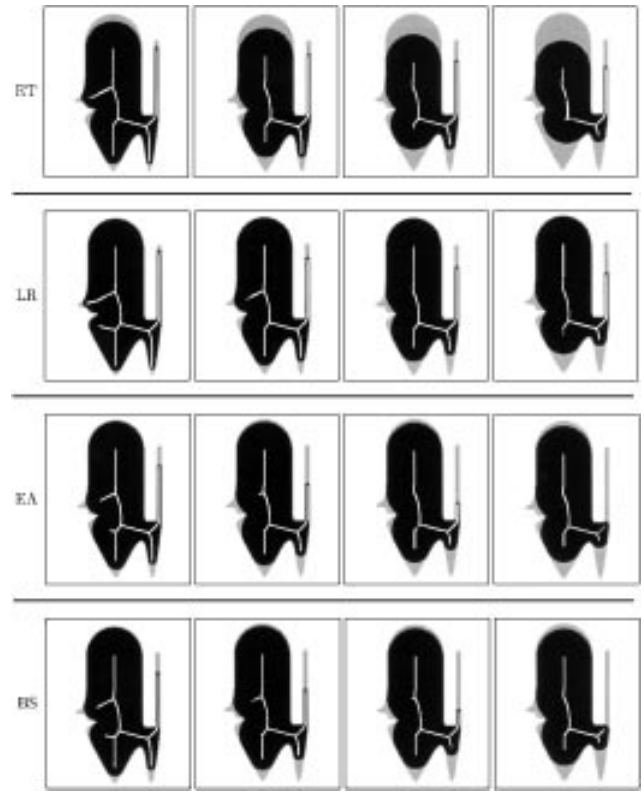

FIG. 11. Results of the pruning algorithms: (ET) erosion thickness; (LR) boundary/ axis length ration; (EA) erosion area; (BS) boundary smoothing based pruning.

The four pruning algorithms we applied are based on the four pruning methods: erosion thickness (ET), boundary/axis length ratio (LR), erosion area (EA), and boundary smoothing-based pruning (BS). In Fig. 11, the simulation results for each pruning method are presented in a separate row. Each row presents four instances of increasingly pruned axes. The gray shapes indicate the original shape and the black shapes are the shapes corresponding to the pruned axes. We tried to present instances of the same pruning degree in the four pruning methods. The rule was: Each instance corresponds to $\frac{1}{5}$, $\frac{2}{5}$, $\frac{3}{5}$, and $\frac{4}{5}$ of the

TABLE 1
Differential Significance Measures

Pruning method	Significance measure	Constant	Wedge ($R(a) = \cos\frac{\phi}{2}$)	Perturb.
Eros. thickness	$1 - R_a$	1	$1 - \cos\frac{\phi}{2}$	$\frac{\alpha^2}{2a^2}$
B/A length ratio	$\frac{1-R_a^2-RR_{aa}}{\sqrt{1-R_a^2}}$	1	$\sin\frac{\phi}{2}$	0
Erosion area	$R\sqrt{1-R_a^2}\cdot(1-R_a)$	R	$R(a)\sin\frac{\phi}{2}(1-\cos\frac{\phi}{2})$	$\frac{\alpha^3}{2a^2}$
Boundary smooth.	$R(1-R_a)$	R	$R(a)(1-\cos\frac{\phi}{2})$	$\frac{\alpha^2}{2a}$

pruning time needed to annihilate the axis segment of the narrow wedge.

From the table and the simulation results in Fig. 11 we make the following observations:

- General:

— As mentioned, the time synchronization across the methods in Fig. 11 is limited. We rescale the time according to the time needed to annihilate a certain axis segment (the segment corresponding to the narrow wedge). However, since the relative significance of axis segments depends on the pruning method, we can have different time correspondences, if we rescale time according to other events.

— Note the uniform erosion thickness in the ET row of the simulation results.

— The eroded boundary length and the erosion area are not so apparent; however, they also seem to be uniform in their corresponding rows of simulation results.

- Constant width:

— The ET and LR pruning methods are invariant to scale. The constant significance value in the constant-width column of the table indicates that wide axes are pruned at the same speed as narrow axes.

— In the EA and BS pruning methods wide axes are more significant than narrow axes, and thus they are pruned slower.

— In the ET row of Fig. 11, the two constant-width axes are pruned at the same rate.

— Equal rate pruning of constant-width axes cannot be noticed in the LR column, because end points of constant-width axes in LR pruning have zero velocity for a time period equal to the length of the circular boundary segment corresponding to the end point, i.e. πR. This time period, is, naturally, shorter for narrow axes and longer for wide axes. Thus the LR pruning may, after all, be considered as scale-dependent.

- Wedge:

— Significance of wedge axis segments is a function of the wedge angle ϕ.

— In the ET and LR rows of Fig. 11, the thin wedge is more significant than the thick wedge.

— Pruned wedge axes are scaled versions of each other (excessively pruned axes are up-scaled versions of moderately pruned axes); Fig. 12.

— Scale dependence may be identified in the EA and BS rows of Fig. 11 during each wedge pruning: the pruning rate is slowed. It may be noticed more easily across axis segments that narrow axes have smaller radius values and are, hence, less significant.

- Small perturbation:

— In the simulation results presented in Fig. 11 the axis segments due to small perturbations are not very long and, thus, should not be expected to correspond to the asymptotic results in the table.

— As noted in the first observation, it is difficult to compare pruning rates from the simulation results in Fig. 11. Still it seems that the ET and EA pruning methods eliminate the small perturbation axes quicker than the other methods.

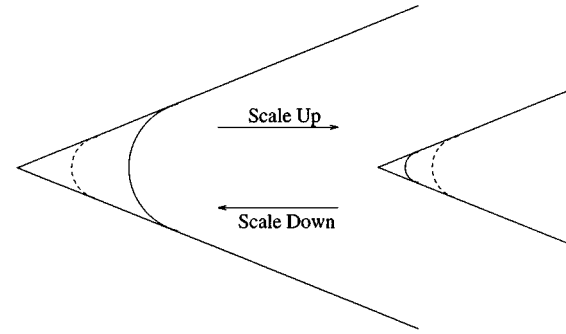

FIG. 12. Pruned wedge axes are scaled versions of each other.

— If the small perturbation is polygonal as in the model (Fig. 10c), the LR differential significance of axis points becomes zero once the axis corresponds to the two vertices (the same vertices correspond to a long axis segment). In this sense the LR method is optimal.

— To analyze the asymptotic results for small perturbation let us return to the threshold prunings corresponding to the different pruning methods. The threshold significance measure is the integral of the differential significance (5). The threshold significance measures corresponding to the ET and EA methods are, therefore, asymptotically similar to $-1/a$, and the threshold significance of the BS method is asymptotically similar to $\log a$. Thus, small perturbation axes are pruned out by the ET and EA methods in finite time, whereas in the BS method they can exist for an arbitrarily long time if they are long enough.

- Inward depression:

— We do not analyze the pruning of axis defects caused by inward depressions because pruning cannot really mend them.

— Usually an inward depression creates two axis segments reaching it from two sides. Those superfluous segments are similar to both segments created by small perturbations and wedge segments.

7.2. Simulation Results

We applied the four pruning methods (ET, LR, EA, BS) to two shapes: Man and Square (see Fig. 13). Both shapes are about 600 pixels wide. Figure 13a is about 350 pixels high, and Fig. 13b is 450 pixels high. The skeletons were obtained using the Curve Axis [40].

In Fig. 14 we present the first pruning hierarchy for each of the methods. The first pruning hierarchy is obtained as follows: First the shape is pruned for a certain time, in our case 10% of the time needed to prune the entire axis. Then parts of the pruned axes get "unpruned." The unpruning process is initiated on every end point of the pruned axis and progresses outward. Unpruning reinstates the axis parts it scans. Arriving at a junction the unpruning process chooses a single branch in which it continues,

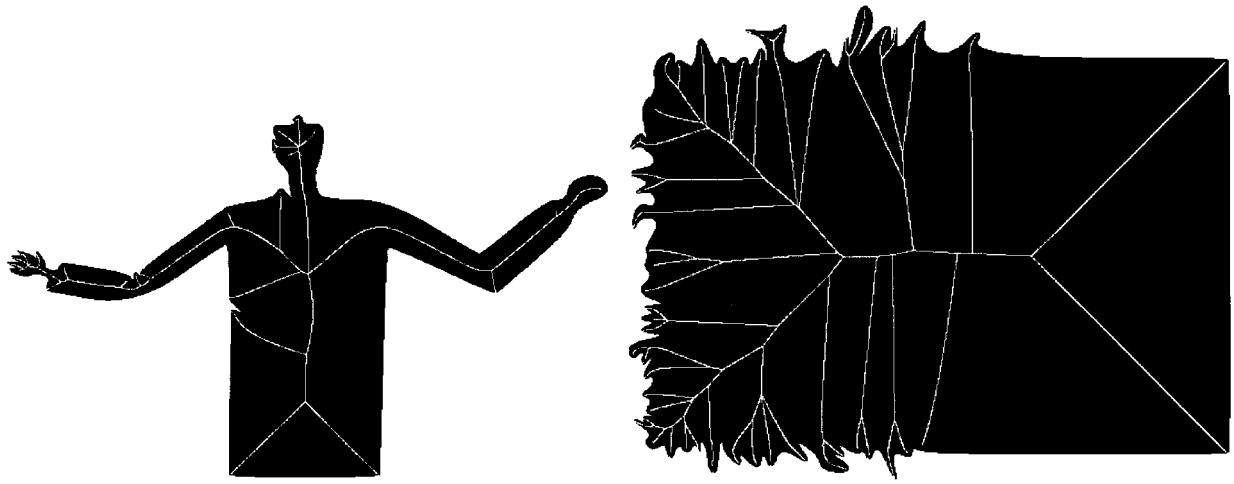

FIG. 13. The two original shapes *man* and *square*, with axes superimposed.

the other branch is not unpruned. From the two branches of a junction, unpruning chooses the branch that lasted longer during the pruning process. Unpruning continues until it tries to unprune a point that was among the earliest to be pruned, in our case less than 2% of the time needed to prune the entire axis.

As already mentioned, the issue of optimal smoothing has not yet been settled. Moreover, in our opinion, optimal smoothing cannot be objectively determined, mainly because human understanding of "reasonable smoothing" is subjective and almost always context-dependent. Thus the goal of this subsection is to point out the different interpretations of smoothing implied by the various pruning methods, rather then to find "the best" method.

The most visible difference in the simulation results of Fig. 14 is between scale-dependent and scale-independent pruning methods. The ET and LR methods are scale-independent, consequently elongated shape protrusions are considered significant no matter how narrow they may be. This might be considered good in shapes like the man shape of Fig. 13a, where relatively small protrusions have contextual meanings of hands and fingers. In context-free shapes as the square shape of Fig. 13b the same feature might be considered a disadvantage.

The difference between the EA and BS methods is usually unnoticeable. In some sense the EA method prunes faster (EA differential significance measure is always smaller than the BS measure since $|R_a| < 1$). The meaning of the above statement is restricted since relative speed depends on how time is scaled. In the presented simulation results the higher pruning rate brought about the pruning of the axis segments corresponding to the base of the man shape by the EA method. One of those segments has been unpruned as can be seen in Fig. 14. The unpruning of this specific segment is due to a negligible difference in the significance measures of the two axis segments. This phenomenon supports the incorporation of the original skeleton hierarchy suggested by Ogniewicz [28, 29] which includes another parameter, enabling the unpruning of two branches in a pruned junction if their significance measures are similar.

We observe that in the LR method occasional groupings of noisy axis branches may seem significant. Note that the unpruned noisy axis branches in the LR pruning of the square shape in Fig. 14 are roots of such groupings. If some of those branches would have terminated in junctions with the main axis rather than joining together before they met the main axis, all of them would have been deleted.

The increased significance of occasional groupings of axis segments is due to the time delay at junctions. At a former junction the pruning process is delayed for a time period equivalent to the boundary length corresponding to the formerly pruned axis segment. Possible modifications to the time delay may alleviate this artifact. The trivial no-delay possibility may cause unduly fast pruning of hairy significant branches; however, replacing the boundary length delay with a chord length delay may be effective. These and other possibilities were not explored.

8. SUMMARY

Pruning methods are incorporated in many skeletonization and thinning algorithms. Although they may seem different, many pruning algorithms are equivalent methods reinvented and restated in a variety of application-dependent formulations. The inconsistent terminology prevents analysis and comparison of the pruning methods.

In this paper we suggested the rate-pruning paradigm as a standard for acceptable pruning methods. Acceptable pruning methods are connected and continuous methods (i.e., resulting axes are connected and pruning is continuous in its degree

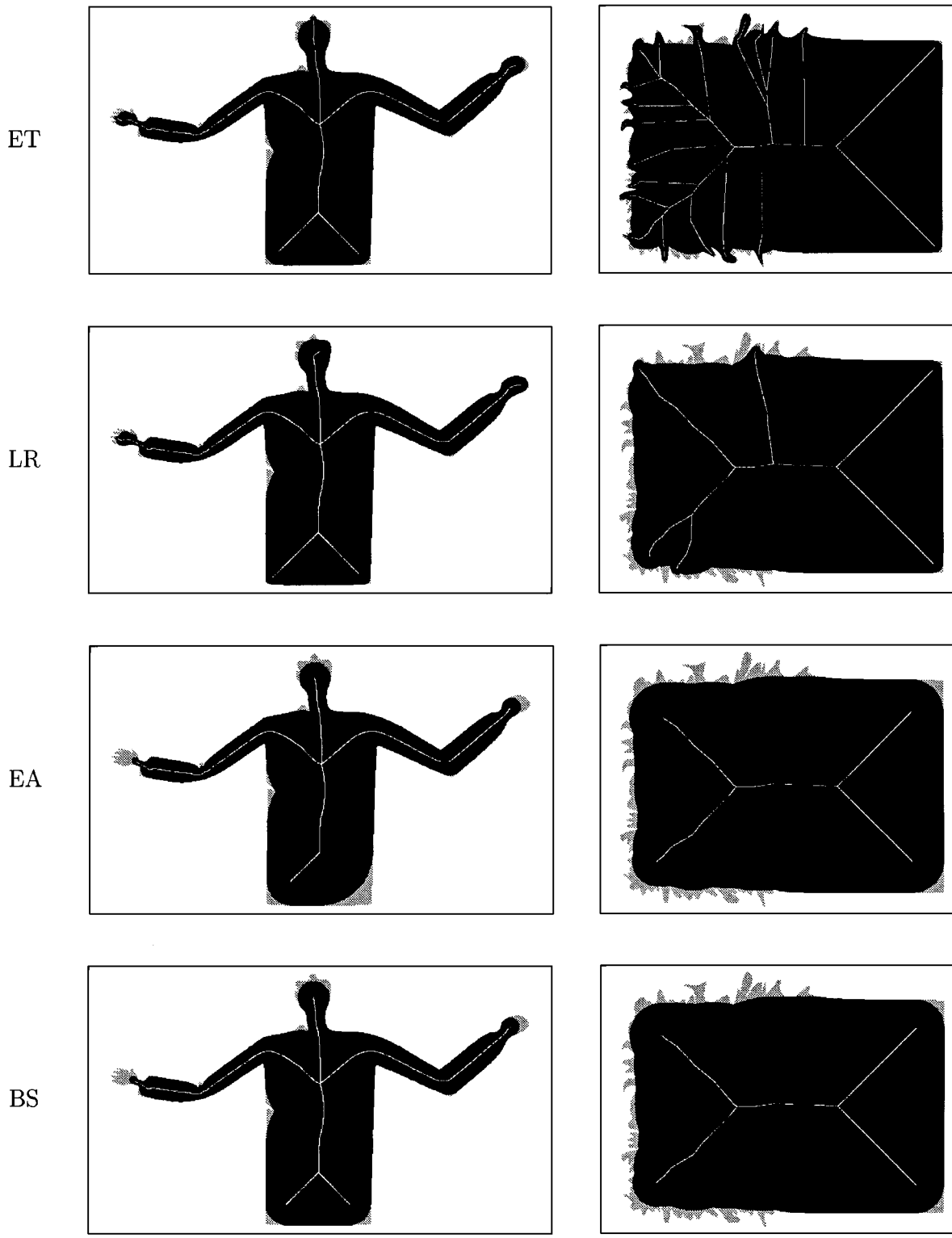

FIG. 14. First pruning hierarchy, pruning large scale details of 10% and unpruning up to small scale details of 2%.

parameter). The standard formulation is a framework in which it is easy to tailor new pruning methods, and we have indeed suggested two new pruning methods: The heuristics behind the proposed *erosion area* pruning is analogous to the heuristics motivating the existing *erosion thickness* method. The second method we proposed is motivated by the curvature flow, a shape-smoothing method which is currently considered as a possible standard for shape smoothing.

In this paper we have also analyzed existing pruning methods. To prove the flexibility of the suggested paradigm and terminology we have reformulated existing acceptable pruning methods in the proposed standard terminology. In the last section we have analyzed and compared the proposed new pruning methods and some of the existing methods and presented their diverse smoothing properties.

Note that we could have proposed the threshold-pruning paradigm as a standard paradigm instead of the potentially more difficult pruning rate paradigm. We did not choose to do so because in this way it would not have been possible to fully standardize the pruning terminology. Identical pruning methods could have been formulated in a variety of heuristic or application-driven global formulations, as was shown to be the case in many publications of existing pruning methods. Using the rate-pruning paradigm it is possible to require truly local formulation of differential significance measure.

The pruning framework proposed in this paper is independent of the skeletonization method applied; however, it does not require its application to be such. One has to keep in mind that in many skeletonization algorithms the radius information is not very accurate. In other applications (e.g., discrete skeletons of small shape parts) the spatial resolution precludes stable derivatives of the radius function. In all those cases, application-specific formulations of the various pruning methods are essential, but should preferably be designed and applied only as stable approximations to the application-invariant formulations.

REFERENCES

1. C. Arcelli, Pattern thinning by contour tracing, *CGIP* **17**, 1981, 130–144.
2. C. Arcelli and G. Sanniti di Baja, A width independent fast thinning algorithm, *IEEE Trans. PAMI* **7**, 1985, 463–474.
3. C. Arcelli and G. Sanniti di Baja, Euclidean skeleton via center of maximal disk extraction, *Image and Vision Computing* **11**, 1993, 163–173.
4. D. Attali and A. Montanvert, Semicontinuous skeletons of 2D and 3D shapes, in *Aspects of Visual Form, Proceedings of the Workshop on Visual Form, May 1994* (C. Arcelli, L. P. Cordella, and G. Sanniti di Baja, Eds.), pp. 32–41, World Scientific, Singapore, 1994.
5. D. Attali, G. Sanniti di Baja, and E. Thiel, Pruning discrete and semicontinuous skeletons, in *Proc. of 8th ICIAP, San Remo, September 1995*.
6. H. Blum, Biological shape and visual science (Part I), *J. Theor. Biol.* **38**, 1973, 205–287.
7. H. Blum and R. N. Nagel, Shape description using weighted symmetric axis features, *Pattern Recognit.* **10**, 1978, 167–180.
8. J. W. Brandt and V. R. Algazi Continuous skeleton computation by voronoi diagram, *CVGIP Image Understanding* **55**, 1992, 329–338.
9. L. P. Cordella and G. Sanniti di Baja, Context dependent smoothing of figures represented by their medial axis transform, in *Proc. of 8th ICPR, 1986*, pp. 280–282.
10. E. R. Davies and A. P. N. Plummer, Thinning algorithms: A critique and a new methodology, *Pattern Recognit.* **14**, 1981, 53–63.
11. A. R. Dill, M. D. Levine, and P. B. Noble, Multiple resolution skeletons, *IEEE Trans. on PAMI* **9**, 1987, 495–504.
12. R. O. Duda and P. E. Hart, *Pattern Classification and Scene Analysis*, Wiley, New York, 1973.
13. M. Gage and R. Hamilton, The shrinking of convex plane curves by the heat equation, *J. of Diff. Geometry* **23**, 1986, 69–96.
14. J. M. Gauch and S. M. Pizer, The intensity axis of symmetry and its application to image segmentation, *IEEE Trans. on PAMI* **15**, 1993, 753–770.
15. C. Gerhardt, Flow of nonconvex hypersurfaces into spheres, *J. of Diff. Geometry* **32**, 1990, 299–314.
16. M. Grayson, The heat equation shrinks embedded plane curves to round points, *J. of Diff. Geometry* **26**, 1987, 285–314.
17. S. Ho and C. R. Dyer, Shape smoothing using medial axis properties, *IEEE Trans. on PAMI* **8**, 1986, 512–520.
18. R. Kimmel, D. Shaked, N. Kiryati, and A. M. Bruckstein, Skeletonization via distance maps and level sets, *CVIU* **62**, 1995, 382–391.
19. F. Leymarie and M. D. Levine, Simulating the grassfire transform using an active contour model, *IEEE Trans. on PAMI* **14**, 1992, 56–75.
20. G. Matheron, Examples of topological properties of skeletons, in *Image Analysis and Mathematical Morphology, Theoretical Advances* (J. Serra, Ed.), Vol. 2, Academic Press, San Diego, 1988.
21. F. Mokhtarian and A. K. Mackworth, Scale-based description and recognition of planar curves and two-dimensional shapes, *IEEE Trans. PAMI* **8**, 1986, 34–43.
22. F. Mokhtarian and A. K. Mackworth, A theory of multiscale, curvature-based shape representation for planar curves, *IEEE Trans. PAMI* **14**, 1992, 789–805.
23. U. Montanari, A method for obtaining skeletons using a quasi-euclidean distance, *J. of the ACM* **18**, 1968, 600–624.
24. U. Montanari, Continuous skeletons from digitized images, *J. of the ACM* **16**, 1969, 534–549.
25. B. Merriman, J. Bence, and S. Osher, *Diffusion Generated Motion by Mean Curvature*, CAM Report 92-18, University of California Los Angeles, April 1992.
26. W. Niblack, P. B. Gibbons, and D. Capson, Generating connected skeletons for exact and approximate reconstruction, in *CVPR Champaign, Illinois, 1992*, pp. 826–828.
27. R. L. Ogniewicz, Automatic medial axis pruning based on characteristics of the skeleton-space, in *Shape Structure and Pattern Recognition, Proc., SSPR Workshop, Nahariya, 1994* (D. Dori and A. M. Bruckstein, Eds.).
28. R. L. Ogniewicz and M. Ilg, Voronoi skeletons: Theory and applications, in *CVPR, Champaign, Illinois, 1992*, pp. 63–69.
29. R. L. Ogniewicz and O. Kübler, Hierarchic Voronoi skeletons, *Pattern Recognit.* **28**, 1995, 343–359.
30. S. Osher and J. A. Sethian, Fronts propagating with curvature-dependent speed: Algorithms based on Hamilton-Jacobi formulation, *J. of Computational Physics* **79**, 1988, 12–49.
31. S. M. Pizer, W. R. Oliver, and S. H. Bloomberg, Hierarchial shape description via the multiresolution symmetric axis transform, *IEEE Trans. PAMI* **9**, 1987, 505–511.
32. J. Ponce, On characterizing ribbons and finding skewed symmetries, *CVGIP* **52**, 1990, 328–340.
33. V. Poty and S. Ubeda, A parallel thinning algorithm using $K \times K$ masks, *J. of Pattern Recognition and Artificial Intelligence* **7**, 1993, 1183–1202.

34. S. Riazanoff, B. Cervelle, and J. Chorowicz, Parameterizable skeletonization of binary and multilevel images, *Pattern Recognition Letters* **11**, 1990, 25–33.

35. A. Rosenfeld, Axial representations of shape, *CVGIP* **33**, 1986, 156–173.

36. A. Rosenfeld and L. S. Davis, A note on thinning, *IEEE Trans. on SMC*, 1976, 226–228.

37. G. Sanniti di Baja, Well-shaped, stable, and reversible skeletons from the (3,4)-distance transform, *J. of Visual Comm. and Image Representation* **5**, 1994, 107–115.

38. J. A. Sethian, Numerical algorithms for propagating interfaces: Hamilton-Jacobi equations and conservation laws, *J. of Diff. Geometry* **31**, 1990, 131–161.

39. D. Shaked, *Symmetry Invariance and Evolution in Shape Analysis*, Ph.D. thesis, Technion, Haifa, Israel, 1995.

40. D. Shaked and A. M. Bruckstein, The curve axis, *CVIU* **63**, 1996, 367–379.

41. J. Serra, *Image Analysis and Mathematical Morphology*, Vol. 1, Academic Press Inc., Orlando Florida, 1982.

42. C. Y. Suen, and P. S. P. Wang, *Thinning Methodologies for Pattern Recognition*, World Scientific, 1994.